

Plasma parameters and stimulated UV emission of filamentary structures in a high-pressure microwave discharge

A. L. Vikharev, A. M. Gorbachev, O. A. Ivanov, and A. L. Kolysko

Applied Physics Institute, Russian Academy of Sciences, 603600 Nizhnii Novgorod, Russia

(Submitted 14 December 1993)

Zh. Eksp. Teor. Fiz. **106**, 172–185 (July 1994)

The fine filaments that develop in a high-pressure microwave discharge in a cylindrically symmetric TE wave due to the growth of the ionization–thermal instability are studied. The discharge parameters are determined by analyzing the linear stage and employing numerical simulation of the discharge evolution, including heating processes and the displacement of the gas in the nonisobaric case. The full gasdynamic description permits the existing results of experimental studies to be extended. It is shown that a plasma filament can emit stimulated UV radiation.

I. INTRODUCTION

Among the different types of gas discharge, the high-pressure microwave discharge in a beam of electromagnetic waves is among those which have been most actively studied in recent years. One reason for this is that such discharges constitute a relatively new topic in gas-discharge physics, which has begun to be studied only after the appearance of high-power microwave generators made from weakly relativistic and relativistic electron beams (including gyrotrons¹). Such nonequilibrium microwave discharges, which are freely localized in space, are of interest for gas-laser technology^{2,3} and plasma chemistry.⁴ In addition to tests of their practical utilization,^{5–8} studies have been made of the complex spatially nonuniform discharge structure that develops at high neutral gas densities (when the frequency of collisions between electrons and molecules is greater than the angular frequency of the microwave field: $\nu > \omega$). Experimental studies^{9–12} have revealed that an originally uniform plasma created within a bounded region of the wave beam decays in the next stage of the discharge into thin (scale lengths on the order of the electromagnetic wavelength λ) filamentary plasma structures elongated in the direction of the electric field. The occurrence of filamentary structure in the discharge is interpreted as the result of the growth of the ionization–thermal instability due to the mutual amplification of perturbations in the electron density and the gas temperature, causing the plasma to decay into filaments parallel to the field.¹³ The magnitude of the instability growth rate (the inverse time for plasma stratification) and the optimum scale length (the separation between filaments) agree fairly well with the experimental data.¹¹

Recently attempts have been made to study the ionization–thermal instability in the nonlinear stage as well. After it is initiated, a filament is predicted theoretically¹⁴ and is shown by experiment¹⁵ to be a time-dependent object in which the plasma parameters grow abruptly. This type of filament development was called by Avetisov *et al.*¹⁵ “ionization collapse.” Experimental studies¹⁵ of the time development of the plasma parameters (electron density and gas temperature) in an individual

filament revealed that the increase in electron density is limited (and the density may even decrease slightly; see Fig. 5 in Ref. 16) in the nonlinear stage of the ionization–thermal instability. This behavior of the electron density implies that the field decreases in the plasma, probably as a result of two mechanisms. One of these is related to broadening of the filament due to gas heating and shielding of the microwave field by its surface layers. The other mechanism is probably due to the wave nature of the interaction between the field and the plasma when the filament is rapidly elongated and it attains longitudinal dimensions comparable with the radiation wavelength. Thus, the suppression of ionization collapse that is established in the experiment in the nonlinear stage of the ionization–thermal instability defines the prospects for using high-pressure microwave discharges to obtain highly nonuniform plasmas.

Regrettably, no reasonably clear theoretical picture of the nonlinear stage in the evolution of a plasma filament exists. Kim and Fraiman¹⁴ studied the nonlinear stage of the ionization–thermal instability in the constant-field approximation. However, the proposed model using a combined treatment of the neutral thermal conduction equation and the electron continuity equation only describes the initial phase of the explosive growth of the parameters in the plasma column. Numerical calculations¹⁷ of the evolution of a microwave discharge at elevated pressure in the field of a converging cylindrical wave employed a simple mathematical model, in which gasdynamic processes were described by means of the isobaric approximation. However, the isobaric approximation (gas pressure given by $p = \text{const}$, i.e., the gas density changes instantaneously as a function of temperature over the whole region where heat is released) does not allow for a faithful description of the discharge dynamics. In the calculations of Ref. 17, this gives rise to a monotonic increase in the electron density and a strong dependence of the discharge dynamics on the margin by which the electric field exceeds the breakdown threshold. On the other hand, in the experiment, e.g., of Ref. 16, after gas breakdown the uniform plasma remains in a quasisteady state for some time (until stratification).

In the present work we study a thin plasma filament arising in the discharge in the microwave field of a cylin-

drically symmetric TE wave. In this wave-field geometry the interaction between the field and the plasma can be described quite simply (in comparison, e.g., with a discharge in a wave beam), which permits us to analyze in detail the time development of the discharge (to find self-consistent spatial distributions of the plasma parameters and the field at different times) in a complete gasdynamic description. Numerical simulation of the discharge dynamics, taking into account heating and displacement of the gas in the nonisobaric case, permits us to generalize the existing results of experimental studies, and to discover new effects associated with the appearance of the plasma filament. Thus, we have shown that ultraviolet (UV) emission can be stimulated from the plasma filament. The efficient generation of UV radiation in a high-pressure discharge shows that its application in plasma chemical reactors for cleansing air of industrial pollution is (e.g., freon) promising. As is well known^{18,19} in order to increase the efficiency of chemical transformations in a nonuniform plasma the use of UV radiation is quite important.

2. EVOLUTION OF A PLASMA FILAMENT

We study the self-consistent evolution of the discharge by means of numerical integration of a system of equations, including equations for the electric field E and the electron density N_e and the gasdynamic equations. The finite velocity with which gasdynamic disturbances propagate is described by the complete system of gasdynamic equations for the velocity \mathbf{v} , density N , and pressure p of the gas with a heating term q :

$$mN\left(\frac{\partial \mathbf{v}}{\partial t} + (\mathbf{v}\nabla)\mathbf{v}\right) = -\nabla p,$$

$$\frac{\partial N}{\partial t} + \text{div}(N\mathbf{v}) = 0, \quad (1)$$

$$\frac{\partial p}{\partial t} + \mathbf{v}\nabla p + \gamma p \text{div} \mathbf{v} = (\gamma - 1)q,$$

where m is the molecular mass and γ is the adiabatic index. Rather than using a specific mechanism for transferring electron energy to the translational degrees of freedom of the gas molecules, we write the heating term q in the form¹⁰

$$q = \delta \sigma E^2, \quad \sigma = \frac{e^2 N_e \nu}{m_e (\omega^2 + \nu^2)}, \quad (2)$$

where δ is the fraction of energy absorbed in the discharge that goes into raising the translational temperature of the gas, and σ is the plasma conductivity.

Neglecting diffusion at high pressure, we can write the equation for the electron density in the form

$$\frac{\partial N_e}{\partial t} = \nu_i(E_e, N) N_e - \nu_a(N) N_e - \alpha N_e^2 - \text{div}(\mathbf{v} N_e). \quad (3)$$

Here ν_a is the electron attachment frequency to the electronegative air molecules, ν_i is the ionization frequency of molecules by electron impact, and α is the electron-ion

recombination coefficient. Over a broad range of parameters ν_i can be approximated as a function of the field by a power of the quantity E/N (Refs. 20 and 21):

$$\nu_i \approx A_1 \left(\frac{E_e}{N}\right)^\beta N, \quad (4)$$

where the exponent has the value $\beta = 4-6$ and the effective field is $E_e = |E| \nu / \sqrt{\nu^2 + \omega^2}$; A_1 is a numerical factor.

In Eq. (3) $\text{div}(\mathbf{v} N_e)$ is the convective term which describes the transport of electrons by the flow of neutral gas.

Consider a discharge in the field of a cylindrically symmetric TE wave (the \mathbf{E} vector is parallel to the axis of symmetry \mathbf{z}_0). In this case the equation for the complex amplitude of the electric field takes the form

$$\frac{\partial^2 E_z}{\partial r^2} + \frac{1}{r} \frac{\partial E_z}{\partial r} + k^2 \hat{\epsilon} E_z = 0 \quad (5)$$

with a complex dielectric function for the discharge plasma given by

$$\hat{\epsilon} = 1 - \frac{N_e}{N_c} \left(1 + i \frac{\nu}{\omega}\right). \quad (6)$$

Here $k = \omega/c$ is the wave number in vacuum, and $N_c = m(\omega^2 + \nu^2)/4\pi e^2 = N_{c0}(1 + \nu^2/\omega^2)$ is the critical value of the electron density.

The system of gasdynamic equations (1) in the geometry we are using can be written in the form

$$mN \left(\frac{\partial v_r}{\partial t} + v_r \frac{\partial v_r}{\partial r} \right) = -\frac{\partial p}{\partial r},$$

$$\frac{\partial N}{\partial t} + \frac{1}{r} \frac{\partial}{\partial r} (r v_r N) = 0, \quad (7)$$

$$\frac{\partial p}{\partial t} + v_r \frac{\partial p}{\partial r} + \gamma p \frac{1}{r} \frac{\partial}{\partial r} (r v_r) = (\gamma - 1)q.$$

We write the boundary conditions for Eqs. (3)–(7) as follows. At $r=0$ (the origin of the coordinate system) we have

$$\left. \frac{\partial N_e}{\partial r} \right|_{r=0} = 0, \quad \left. \frac{\partial E_z}{\partial r} \right|_{r=0} = 0, \quad \left. \frac{\partial N}{\partial r} \right|_{r=0} = 0, \quad (8)$$

$$\left. \frac{\partial p}{\partial r} \right|_{r=0} = 0, \quad v_r|_{r=0} = 0.$$

Outside the discharge region at $r=R$ we have

$$\left. \frac{\partial N_e}{\partial r} \right|_{r=R} = 0, \quad \left. \frac{\partial N}{\partial r} \right|_{r=R} = 0, \quad \left. \frac{\partial p}{\partial r} \right|_{r=R} = 0, \quad (9)$$

$$\left. \frac{\partial v_r}{\partial r} \right|_{r=R} = 0.$$

The electromagnetic wave field in the region $r \geq R$, where $N_e = 0$ and $\hat{\epsilon} = 1$ hold, is represented as the sum of an incident (convergent) and a reflected (divergent) cylindrical wave, satisfying the conditions

$$E_z(R) = AH_0^{(1)}(kR) + G_{\text{ref}} AH_0^{(2)}(kR), \quad (10)$$

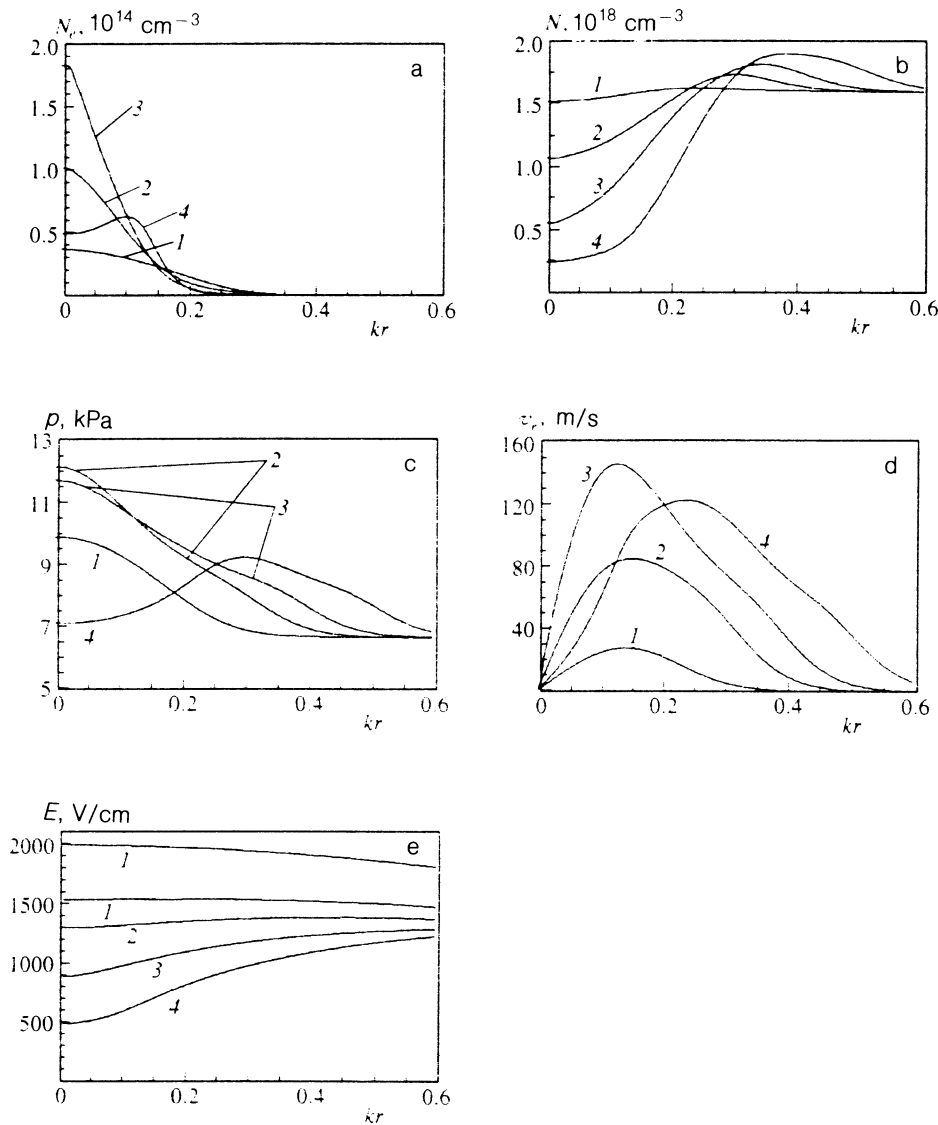


FIG. 1. Space-time evolution of the electron density N_e (a), gas density N (b), pressure p (c), velocity V_r (d), and the magnitudes of the electric field $|E|$ (e) at times (in μs): 1) 0; 2) 5.5; 3) 6.4; 4) 8.

$$\left. \frac{\partial E_z}{\partial r} \right|_{r=R} = A \left. \frac{\partial H_0^{(1)}}{\partial t} \right|_{r=R} + G_{\text{ref}} A \left. \frac{\partial H_0^{(2)}}{\partial t} \right|_{r=R},$$

where $H_0^{(1)}(kr)$ and $H_0^{(2)}(kr)$ are Hankel functions of the first and second kind, respectively, describing the convergent and divergent waves in vacuum, A is the amplitude of the incident wave, assumed to be a specified quantity, and G_{ref} is the complex reflection coefficient. If there is no plasma we have $\hat{\epsilon} = 1$ throughout all of space, and Eq. (5) together with conditions (8) and (10) has a solution in the form of a cylindrical standing wave:

$$E_z(r) = E_0 J_0(kr), \quad E_0 = 2A, \quad G_{\text{ref}} = 1, \quad (11)$$

where $J_0(kr)$ is a Bessel function of the first kind.

The initial conditions for the system of equations were as follows:

$$N(r,0) = N_0, \quad v(r,0) = 0, \quad p(r,0) = p_0, \quad (12)$$

$$N_e(r,0) = N_{e0} \ll N_{c0},$$

$$p = N k_B T, \quad (13)$$

where k_B is the Boltzmann constant and T is the absolute gas temperature (the initial temperature was $T_0 = 300$ K).

The calculations were performed for air and a microwave wavelength (in vacuum) $\lambda = 3$ cm; the various parameters of Eqs. (3)–(7) assumed the following values:¹⁰

$$N_{c0} = 10^{12} \text{ cm}^{-3}, \quad \nu [\text{s}^{-1}] = 1.5 \cdot 10^{-7} \cdot N [\text{cm}^{-3}], \quad (14)$$

$$\nu_a = 10^{-5} \cdot \nu, \quad \alpha = 2 \cdot 10^{-8} \text{ cm}^3/\text{s}.$$

The ionization frequency ν_i was determined by approximating the experimental and calculated plots given in Ref. 22. The fraction of the energy (2) converted into heat was assumed to be $\delta = 0.1$ (Ref. 23).

The results of the calculations¹⁾ are shown in Figs. 1 and 2. Qualitatively, the space-time evolution of the discharge did not depend on the initial gas pressure, and can be expressed as follows. In the initial stage we observe avalanche growth of the electron density in the region of maximum field near the discharge axis (Fig. 1a, trace 1; Fig. 2a, trace 2). After the electron density reached a high enough value, due to screening of the field by the plasma

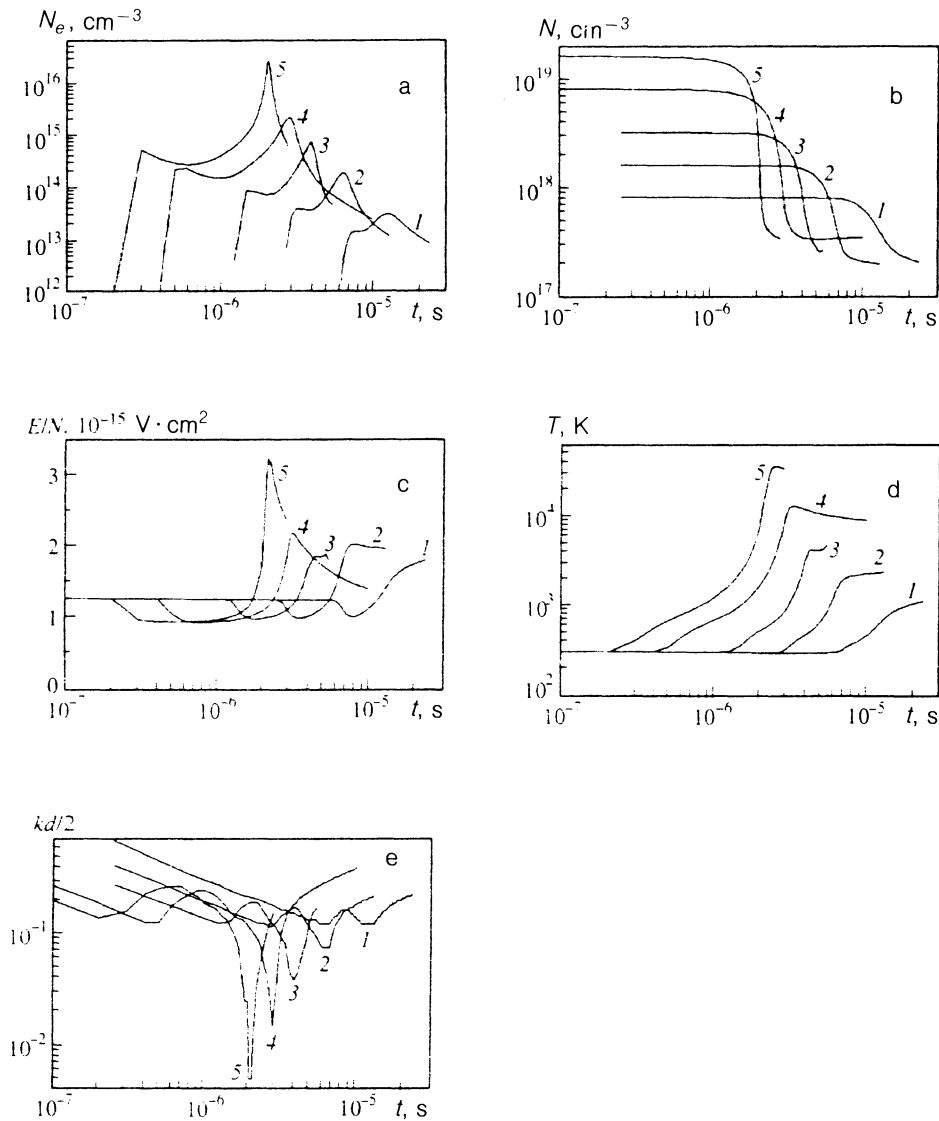


FIG. 2. Time dependence of the electron density N_e (a), gas density N (b), the parameter E/N (c), the gas temperature T (d), on the discharge axis (for $kr=0$) and the characteristic half-width at half maximum of the electron distribution (e) $E_0/N_0=1.2 \cdot 10^{-15} \text{ V} \cdot \text{cm}^2$ ($E_0/p_0=40 \text{ V} \cdot \text{cm}^{-1} \cdot \text{torr}^{-1}$). In the figures the labels denote the different initial pressures: (torr): 1) 25; 2) 50; 3) 100; 4) 250; 5) 500.

(Fig. 1e, trace 1; Fig. 2c) the discharge went over to a quasisteady state accompanied by some broadening of the region occupied by the uniform plasma (Fig. 2e) and a slight decrease in the electron density (Fig. 2a). During this time the gas heated and its pressure rises (Fig. 2c, traces 1 and 2; Fig. 2d). However, due to the inertia of the gas the expansion rate is small at the start of heating (Fig. 1d, traces 1 and 2) and the density in the quasisteady state of the discharge remains practically unchanged (cf. Fig. 2b and Fig. 2d). Consequently, a plateau develops in the function $N_e(t)$ (Fig. 2a), which is absent in calculations in the isobaric approximation¹⁷ where the gas density decays simultaneously with the heating.

As the gas expansion rate approaches the speed of sound, the gas density begins to decrease in the central region of the discharge (Fig. 1b and Fig. 2b), and the ionization-thermal instability develops. Despite the decay of the field due to the rise in the plasma density (Fig. 1e), the drop in the gas density increases the value of the parameter E/N (Fig. 2c) and rapidly raises the electron density (Fig. 1a, trace 3; Fig. 2a). The electron density in-

creases near the discharge axis; the characteristic radius of the electron density profile decreases sharply (cf. traces 1 and 3, Fig. 1a and Fig. 2e), and a thin plasma filament develops. The instability stops growing due to the decrease in the effective field E_e as the gas density drops to a level at which the electron collision frequency becomes close to the frequency of the field, $\nu \approx \omega$. Thereafter the filament spreads out (Fig. 2e), accompanied by a decay of the field and the electron density (Fig. 1a, trace 4; Fig. 2a, c).

The numerical simulation revealed that the filament evolution and its parameters in the nonisobaric case depend weakly on the initial value of E_0/N_0 . The reason for this is the rapid transition of the discharge to the quasisteady state with a quasiuniform plasma having similar parameters, with almost the same electron density and hence retarding field. Naturally the gas heating is the same, provided that it is small during the breakdown stage. The opposite behavior was observed in the numerical simulation¹⁷ in the isobaric approximation, where the time dependence of the discharge depends strongly on the amplitude of the incident wave. For small values of the field

the gas heating has a significant effect on the discharge dynamics, while at large amplitudes the heating and the decrease in gas density are only an additional factor, and the discharge dynamics are similar to the unheated regime.²⁴

As can be seen from Fig. 2, the dependence of the plasma parameters on the initial gas pressure is very sensitive. As the gas pressure increases, the rate at which the filament diameter decreases, and consequently the maximum electron density, the parameter E/N , and the gas temperature increase.

We note one additional aspect of the evolution of a plasma filament. Ionization is a very fast process, so the electron density tracks the change in E/N in a quasisteady way; on the other hand, the electric field strength in the filament is determined by the electron density. Thus, E/N can be estimated using

$$v_i(|E_e|, N) = \alpha N_e, \quad (15)$$

which yields values close to those calculated.

Summarizing the main properties of the dynamics of a plasma filament, we emphasize that the filament is a non-steady rapidly developing nonlinear phenomenon, small in size, and has high values of electron density and gas temperature. The filament parameters depend sensitively on the initial density (pressure) of the gas and weakly on the electric field amplitude.

3. UV RADIATION FROM A PLASMA FILAMENT

As already noted, the occurrence of a plasma filament in a microwave discharge is accompanied by an increase in E/N and the electron density N_e . Under these conditions the efficiency with which electronic states of the molecules are excited rises, and it is possible to produce a population inversion and to obtain a situation in which radiation is amplified along the filament.

In the present work the power of the spontaneous and stimulated emission per unit volume is estimated using a simplified kinetic model describing the operation of a nitrogen laser $C^3\Pi_u - B^3\Pi_g$, transition, 0-0 band, $\lambda_2 = 337.1$ nm) analogous to that performed in Ref. 25. We supplement Eqs. (3)–(7) with the rate equations for the populations in the upper $N_c(v=0)$ and lower $N_b(v=0)$ laser levels and the photon density N_{ph} :

$$\begin{aligned} \frac{\partial N_c}{\partial t} &= k_c N N_e - \frac{N_c}{\tau_c} - \sigma_a c (N_c - N_b) N_{ph} - k_{cn} N_c \\ &\quad \times N - k_{ec} N_c N_e, \\ \frac{\partial N_b}{\partial t} &= k_b N N_e - \frac{N_b}{\tau_b} + \sigma_a c (N_c - N_b) N_{ph} - k_{bn} \\ &\quad \times N_b N - k_{eb} N_b N_e, \\ \frac{\partial N_{ph}}{\partial t} &= \psi \frac{N_c}{\tau_c} + \sigma_a c (N_c - N_b) N_{ph} - \frac{N_{ph}}{\tau_{ph}}, \end{aligned} \quad (16)$$

where τ_c , τ_b , τ_{ph} are the radiative lifetimes of the laser levels and of the photons in the discharge; k_{cn} , k_{bn} , k_{ec} , k_{eb} are the quenching rates for these levels associated with

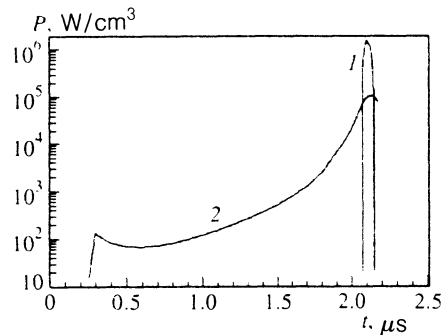


FIG. 3. Time dependence of the specific power of the stimulated emission $P_{ind} = h\nu\sigma c(N_c - N_b)N_{ph}$ (1) and the spontaneous emission $P_s = h\nu\psi N_c/\tau_b$ (2) parallel to the axis of the plasma filament, corresponding to traces 5 in Fig. 2.

molecular and electron collisions respectively; σ_a is the absorption cross section; ψ is a coefficient that takes into account the directionality of the stimulated emission $\psi = d/l$ (d is the filament diameter and l is its length, which we assume in the calculations approximately equal to $\lambda/2$). The magnitudes of the constants that enter into the equations were chosen based on the results of Refs. 26 and 27. The constants for the excitation of the $N_c(v=0)$ and $N_b(v=0)$ levels by electron impact were calculated by the method given in Ref. 26. This assumption is completely valid in the case when the electron density in the discharge is high and collisions between electrons play a major role in the formation of the distribution function.

Calculations²⁾ showed that as a result of the formation of the filament, the specific power in spontaneous emission increases severalfold. At high pressures ($p_0 \geq 500$ torr) the filament diameter is quite small; consequently, the electron density is large and the parameter E/N reaches large values for which population inversion and induced emission from the plasma filament are possible (Fig. 3).

4. DISCUSSION OF RESULTS AND COMPARISON WITH THE EXPERIMENTAL DATA

These numerical results can serve as control and reference points for estimating the diameter and electron density of a plasma filament by means of linear analysis and simple qualitative considerations.

In the linear stage of instability growth, when a filament is born with diameter d much less than the wavelength λ , and with filaments separated by a distance Λ , we will neglect the variations in the field, assuming it to be uniform. On the one hand this simplifies the problem, while on the other it allows us to make clearer the role of the gasdynamic processes described by Eqs. (1) in the formation of the filament. We write the equation for the electron density in a form simpler than (3):

$$\frac{\partial N_e}{\partial t} = \nu_i N_e - \nu_a N_e. \quad (17)$$

We will assume that the electron collision frequency ν is proportional to the gas density N . At high pressures when $\nu \gg \omega$ holds, we have $E_e \approx |E|$, and Eqs. (2) and (4) can be rewritten in the form

$$q = k_1 N_e / N, \quad (18)$$

$$\nu_i = k_2 N^{-\varphi}, \quad \varphi = \beta - 1, \quad (19)$$

where k_1 and k_2 are constants independent of N and N_e .

Next, we will assume that the uniform gas heating is slow, so that we have

$$\zeta_0 = \frac{1}{p} \frac{\partial p}{\partial t} = (1 - \gamma) \frac{q}{p} \ll \xi_m, \quad (20)$$

where ξ_m is the maximum instability growth rate and ζ_0 is the reciprocal of the time for uniform heating of the gas with $N = \text{const}$. In this case Eqs. (1), (17)–(19) have a time-independent solution for some value of the electric field:

$$N = N_0, \quad p = p_0, \quad v = 0, \quad N_e = N_{e0}, \quad \nu_{i0} = \nu_a. \quad (21)$$

The condition for the nontrivial solubility for perturbations of the form $\exp(\xi t - i\eta x)$ of the set of equations (1), (17) about (21) yields the dispersion relation

$$\xi^4 + c_s^2 \eta^2 \xi^2 - \frac{\eta^2}{m} (A\xi + BC) = 0, \quad (22)$$

where

$$A = -(\gamma - 1) \frac{\partial q}{\partial N} = (\gamma - 1) \frac{q_0}{N_0}, \quad (23)$$

$$B = (\gamma - 1) \frac{\partial q}{\partial N_e} = (\gamma - 1) \frac{q_0}{N_{e0}}, \quad (24)$$

$$C = -N_{e0} \frac{\partial(\nu_i - \nu_a)}{\partial N} = \varphi \nu_{i0} \frac{N_{e0}}{N_0}, \quad (25)$$

$c_s = \sqrt{\gamma p_0 / \rho_0}$ is the speed of sound, and $\rho_0 = m N_0$ is the initial density of the gas. For $A = B = C = 0$ we have $\xi = \pm i c_s \eta$, i.e., ordinary sound waves.

The term $A\xi$ describes the increase in the power of the source resulting from the variation of the gas density, while BC is the increase in the power associated with the rise in the electron density. Consider the case for which

$$A\xi_m \ll BC, \quad (26)$$

then Eq. (22) has the form of a readily soluble biquadratic equation:

$$\xi^4 + c_s^2 \eta^2 \cdot \xi^2 - \frac{\eta^2 BC}{m} = 0, \quad (27)$$

which has one real positive solution:

$$\xi = \left[\frac{\sqrt{c_s^4 \eta^4 + 4\eta^2 BC/m} - c_s^2 \eta^2}{2} \right]^{1/2}. \quad (28)$$

Figure 4 shows a plot of $\xi^2 = \xi^2(\eta^2)$ for this case. In the figure we have set

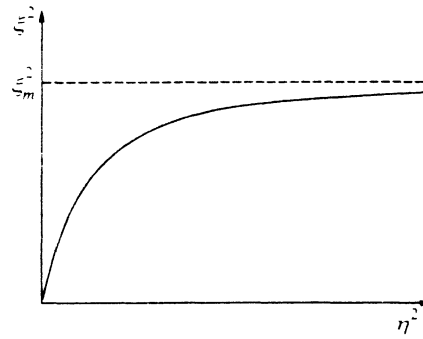


FIG. 4. Instability growth rate ξ versus the wave number η .

$$\xi_m^2 = \frac{BC}{c_s^2 m} = \varphi(\gamma - 1) \frac{q_0}{p_0} \nu_{i0} = \varphi \zeta_0 \nu_{i0}. \quad (29)$$

Then conditions (20) and (26) together with (29) and (23)–(25) take the form

$$\zeta_0 = (\gamma - 1) \frac{q_0}{p_0} \ll \varphi \nu_{i0}. \quad (30)$$

Relation (30) is usually satisfied under experimental conditions.

Expression (29) for the instability growth rate is close to that given in Refs. 10 and 13 for the isobaric approximation in a prescribed field for small values of the gas thermal conductivity and electron diffusion. It is possible to neglect the diffusion in Eq. (17) under the condition

$$\xi_m \gg D/d^2, \quad (31)$$

where D is the electron ambipolar diffusion coefficient and d is the diameter of the plasma filament.

The plot of $\xi^2 = \xi^2(\eta^2)$ (Fig. 4) is qualitatively similar to the analogous dependence obtained in Ref. 28 for a glow discharge. Thus, in a dense gas in a microwave discharge, just as in a glow discharge, the small-scale perturbations have the largest growth rate.

Let us use these relations to estimate the maximum electron density $N_{e \text{ max}}$ and the diameter of the plasma filament and compare them with the results of the numerical calculations and experiments.

The time for creating a filament found in the numerical calculation agrees with the estimate according to Eq. (17). The filament diameter (Fig. 2e) is determined by the distance over which a disturbance in the gas density propagates in the time required for the filament to form, and can be estimated in terms of $\eta_0 = \xi_m / c_s$ [see Fig. 4 and Eq. (29)]:

$$d = \frac{2\pi}{\eta_0} = \frac{2\pi c_s}{\sqrt{\varphi \eta_0 \nu_{i0}}}. \quad (32)$$

Knowing the diameter d of the plasma filament, we can estimate the maximum electron density. It follows from the calculations that $N_{e \text{ max}}$ is such that the field of the electro-

magnetic waves penetrates deeply into the plasma filament. This is valid if the thickness of the filament is less than or of the order of the skin depth:

$$d \lesssim \frac{c}{\sqrt{2\pi\sigma\omega}}. \quad (33)$$

We obtain further simplifications if we take into account that the instability grows until the gas density N drops to the level $\nu \approx \omega$. Then using (2) and (6) we can rewrite (33) in the form

$$N_{e \max} \leq N_{c0}(kd)^{-2}. \quad (34)$$

The results of the estimates made using Eqs. (32) and (34) agree fairly well with the results of the numerical calculations (Fig. 2).

Thus, gasdynamic processes associated with the creation of a filament determine its penetration time and diameter, and these in turn are what determine the maximum electron density and the value of E/N .

The comparison between the results of these calculations and the evolution of the electron density and gas temperature in a plasma filament observed in experiment¹⁶ reveals the following. With the plasma parameters $\lambda = 4$ cm, $\rho_0 = 50$ torr, $N_{e0} \approx 10^{13}$ cm⁻³, $E_0 = 2$ kV/cm, $\nu_0 \approx 2 \cdot 10^7$ s⁻¹ the numerical model describes the evolution of the electron density in the filament fairly well both qualitatively and quantitatively. From Eqs. (29), (32), and (34) we find the estimates

$$\begin{aligned} 1/\xi_m &\approx 7 \cdot 10^{-7} \text{ s}, \quad d \approx 1.5 \text{ mm}, \\ N_{e \max} &\leq 2 \cdot 10^{14} \text{ cm}^{-3}, \end{aligned} \quad (35)$$

which also agree well with the experimental data. On the other hand, the agreement between the time dependence of the gas temperature in the calculation and in the experiments is only order-of-magnitude (we can compare $T \approx 10^3$ K from Ref. 16 with the plots in Fig. 2d).

It should also be noted that the calculations in the nonisobaric case agree with the experimentally observed strong dependence of the electron density on the initial gas pressure and the weak dependence on the electric field amplitudes.^{15,29} The results of the estimates made from Eqs. (29), (32), and (34) for the conditions of the experiment in Ref. 15 in argon are in satisfactory agreement with the measured data. With the experimental parameters $\lambda = 2$ cm, $p_0 = 200$ torr, $E_0 \approx 2.7$ kV/cm, we take the initial (prior to the onset of the ionization-thermal instability) electron density to be the same as in the numerical calculation, i.e., $|\varepsilon| \approx 1$, $N_{e0} \approx 5 \cdot 10^{13}$ cm⁻³, the fraction of the energy transformed into heat for a monotonic gas to be $\delta \approx 1$, and we assume $\nu/\omega \approx 15$, as a result of which we find $q \approx 8 \cdot 10^4$ W/cm³, $\nu_0 \approx 10^8$ s⁻¹, and the following parameters for the plasma filament:

$$\begin{aligned} 1/\xi_m &\approx 5 \cdot 10^{-8} \text{ s}, \quad d \approx 8 \cdot 10^{-3} \text{ cm}, \\ N_{e \max} &\leq 5 \cdot 10^{15} \text{ cm}^{-3}. \end{aligned} \quad (36)$$

Note that the effects of gas thermal conductivity on the dynamics and parameters of the filaments are outside the scope of this model. At such high gas temperatures, ther-

mal ionization and dissociation can contribute significant corrections. Thus, following Ref. 30 for $p = 1$ atm and $T = 10^4$ K the equilibrium electron density is $N_e \approx 10^{16}$ cm⁻³, which is close to that found in the calculation (Fig. 2a). The effect of these processes on the dynamics and parameters of the plasma filament remains an open question.

5. CONCLUSION

In this work we have reported the results of numerical simulations of the evolution of a high-pressure microwave discharge in air in the field of a cylindrically symmetric TE wave, including the heating and expulsion of the gas in the nonisobaric case. We have employed a simple geometry for the wave field in the calculations; nevertheless, the full gasdynamic description enabled us to model the basic behavior of the time-dependent microwave discharge at high pressure observed experimentally in wave beams. The following stages have been established for the development of a microwave discharge in air: the existence of a quasisteady discharge phase with a uniform plasma, the creation of a plasma filament due to the growth of the ionization-thermal instability in the plasma, and saturation of the electron density in the plasma filament due to nonlinear processes. The parameters of the plasma filament in the nonlinear stage of the ionization-thermal instability are determined primarily by the initial pressure (or density) of the gas and depend weakly on the amplitude of the electric field. In the calculations we have obtained both qualitative and quantitative agreement with experiment (the numerical values and the behavior of the plasma variables of the filament as a function of field strength and pressure).

Study of the space-time evolution of the discharge reveals that the electric field is expelled from the plasma filament due to the skin phase in the initial stage of filament creation, but this does not limit the increase in electron density, since E/N grows despite the decrease in field. Only when the gas density in the film reaches a level such that $\nu \approx \omega$ holds does N_e stop growing due to the skin effect.

We have shown that at sufficiently high gas pressures the electron density and the quantity E/N (electron temperature) cause the plasma filament to become an intense source of UV radiation. Under some conditions it is even possible to obtain stimulated emission from the plasma filament.

In this work we have suggested simple relations for estimating the parameters of the plasma filament (the maximum electron density and diameter). In the linear analysis, the use of the nonisobaric description of the gasdynamic processes enabled us to find the characteristic length scale and the diameter of the plasma filament, and hence to determine the electron density and the parameter E/N .

In conclusion we wish to express our gratitude to the participants of the seminar of A. G. Litvak for critical comments and fruitful discussions. We note also that this work was performed with financial support from the Russian Fund for Theoretical Investigation (Project No. 93-02-846).

¹⁾Equations (3) and (7) were solved using a simple explicit scheme, while Eq. (5) was solved by an explicit two-step method that yields very smooth solutions. From the boundary conditions (10) we determined the reflection coefficient G_{ref} ; then the field strength in the plasma was chosen so that the amplitude of the incident wave was equal to A .

²⁾Equation (16) was solved separately from Eqs. (3)–(7) using the Euler scheme with a variable time step. The functions $N(t)$, $E(t)$, and $N_e(t)$ were approximated using the results of solving Eqs. (3)–(7).

¹V. A. Flyagin, A. V. Gaponov, M. I. Petelin, and V. K. Yulpatov, *IEEE Trans. Microwave Theory Tech.* **25**, 514 (1977).

²G. M. Batanov, I. A. Kossyi, and G. S. Luk'yanchikov, *Zh. Tekh. Fiz.* **50**, 346 (1980) [*Sov. Phys. Tech. Phys.* **25**, 204 (1980)].

³A. L. Vikharev, O. A. Ivanov, and A. V. Kim, in *Relativistic High-Frequency Electronics*, A. V. Gaponova-Grekhov (ed.) [in Russian], Applied Physics Institute, USSR Academy of Sciences, Gorkii (1990), Issue 6, p. 256.

⁴V. D. Rusanov and A. A. Fridman, *Physics of Chemically Activated Plasma* [in Russian], Nauka, Moscow (1984).

⁵Yu. V. Bykov, *Khim. Vys. Énerg.* **18**, 347 (1984).

⁶Yu. V. Bykov, S. V. Golubev, A. L. Gol'denburg, and V. G. Zorin, *Zh. Tekh. Fiz.* **54**, 723 (1984) [*Sov. Phys. Tech. Phys.* **29**, 428 (1984)].

⁷S. I. Gritsinin, L. V. Kolik, I. A. Kossyi *et al.*, *Zh. Tekh. Fiz.* **58**, 2293 (1988) [*Sov. Phys. Tech. Phys.* **33**, 1399 (1988)].

⁸G. A. Askar'yan, G. M. Batanov, S. I. Gritsinin *et al.*, *Zh. Tekh. Fiz.* **60**, 77 (1990) [*Sov. Phys. Tech. Phys.* **35**, 1275 (1990)].

⁹G. M. Batanov, S. I. Gritsinin, I. A. Kossyi *et al.*, in *Transactions of the Lebedev Institute*, Vol. 160 [in Russian], Nauka, Moscow (1985), p. 41.

¹⁰A. L. Vikharev, V. B. Gil'denburg, A. V. Kim *et al.*, in *High-Frequency Discharge in Wave Fields*, A. G. Litvak (ed.) [in Russian], Plasma Physics Institute, USSR Academy of Sciences, Gor'kii (1988), p. 41.

¹¹A. L. Vikharev, V. B. Gil'denburg, S. V. Golubev *et al.*, *Zh. Eksp. Teor. Fiz.* **94**(4), 136 (1988) [*Sov. Phys. JETP* **67**, 724 (1988)].

¹²L. P. Griachev, I. I. Esakov, G. I. Mishin, and A. B. Fedotov, *Zh. Tekh. Fiz.* **59**(10), 149 (1989) [*Sov. Phys. Tech. Phys.* **34**, 1181 (1989)].

¹³V. B. Gil'denburg and A. V. Kim, *Fiz. Plazmy* **6**, 904 (1980) [*Sov. J. Plasma Phys.* **6**, 496 (1980)].

¹⁴A. V. Kim and G. M. Fraiman, *Fiz. Plazmy* **9**, 613 (1983) [*Sov. J. Plasma Phys.* **9**, 358 (1983)].

¹⁵V. G. Avetisov, S. I. Gritsinin, A. V. Kim *et al.*, *Pis'ma Zh. Eksp. Teor. Fiz.* **51**, 306 (1990) [*JETP Lett.* **51**, 348 (1990)].

¹⁶A. L. Vikharev, A. M. Gorbachev, A. V. Kim *et al.*, *Fiz. Plazmy* **18**, 1064 (1992) [*Sov. J. Plasma Phys.* **18**, 884 (1992)].

¹⁷I. B. Bokolishvili, A. V. Kim, G. G. Malinetskii *et al.*, Preprint No. 76, Institute for Problems in Mechanics, USSR Academy of Sciences, Moscow (1989).

¹⁸A. P. Shvedchikov, É. V. Belousova, A. V. Polyakova *et al.*, *Khim. Vys. Énerg.* **26**, 317 (1992).

¹⁹M. B. Chang, J. H. Balbach, M. J. Rood *et al.*, *J. Appl. Phys.* **69**, 4409 (1991).

²⁰J. T. Mayhan, R. L. Fante, R. O'Keefe *et al.*, *J. Appl. Phys.* **42**, 5362 (1971).

²¹A. V. Gurevich, *Geomagn. Aeron.* **19**, 633 (1979).

²²A. L. Vikharev, O. A. Ivanov, A. N. Stepanov *et al.*, in *High-Frequency Discharges in Wave Fields*, A. G. Litvak (ed.) [in Russian], Applied Physics Institute, USSR Academy of Sciences, Gor'kii (1988).

²³A. V. Berdyshev, A. L. Vikharev, M. S. Gitlin *et al.*, *Teplotiz. Vys. Temp.* **26**, 661 (1988).

²⁴I. B. Bokolishvili, A. V. Kim, G. G. Malinetskii *et al.*, Preprint No. 155, Institute of Problems in Mechanics, USSR Academy of Sciences, Moscow (1989).

²⁵W. A. Fitzsimmons, L. W. Anderson, C. E. Riedhauser *et al.*, *IEEE J. Quantum Electron.* **QE-12**, No. 10, 624 (1976).

²⁶Y. Itikawa, M. Hayashi, A. Ichimura *et al.*, *J. Chem. Phys. Ref. Data* **15**, No. 3, 985 (1986).

²⁷L. G. Christophorow, *Electron-Molecular Interactions and Their Application*, Vol. 1, Academic, New York (1984).

²⁸E. P. Velikhov, V. D. Pis'mennyi, and A. T. Rakhimov, *Usp. Fiz. Nauk* **122**, 419 (1977) [*Sov. Phys. Usp.* **20**, 586 (1977)].

²⁹V. V. Zlobin, A. A. Kuzvinokov, and V. M. Shibkov, *Bull. Moscow State Univ., Ser. 3, Phys. Astron.* **29**, No. 1, 89 (1988).

³⁰Yu. P. Raizer, *Gas-Discharge Physics*, Springer, New York (1989).

Translated by David L. Book